EPJ D
Atomic, Molecular, Optical and Plasma Physics
EPJ.org
your physics journal

Eur. Phys. J. D **59**, 233–240 (2010) DOI: 10.1140/epjd/e2010-00158-8

Solid-state traveling-wave amplifiers and oscillators in the THz range: effect of electron collisions

O. Sydoruk, E. Shamonina and L. Solymar

EDP SCIENCES
Società Italiana di Fisica
Springer

Eur. Phys. J. D **59**, 233–240 (2010)
DOI: 10.1140/epjd/e2010-00158-8

THE EUROPEAN PHYSICAL JOURNAL D

Regular Article

Solid-state traveling-wave amplifiers and oscillators in the THz range: effect of electron collisions

O. Sydoruk[1,a], E. Shamonina[2], and L. Solymar[1]

[1] Department of Electrical and Electronic Engineering, Optical and Semiconductor Devices Group, Imperial College, London Exhibition Road, London SW7 2AZ, UK
[2] Erlangen Graduate School in Advanced Optical Technologies, University of Erlangen-Nuremberg, Paul-Gordan-Str. 6 91052, Erlangen, Germany

Received 12 April 2010
Published online 11 June 2010 –

Abstract. Due to their high plasma frequencies, drifting semiconductor plasmas interacting with slow electromagnetic waves hold promise for terahertz amplifiers and oscillators. In these devices, the gain and the type of instabilities are influenced by electron collisions. To study the effect of collisions, we developed a two-wave model describing the interaction between drifting solid-state plasmas and electromagnetic waves. This paper analyzes the two-wave dispersion relation for representative examples. As the examples show, convective and absolute instabilities can occur at high and low collision frequencies depending on the relationship between the collision frequency and the coupling coefficient. Surprisingly, an absolute instability occurs when collision-dominated plasmas interact with backward waves. The model can be used to determine the potential of a particular configuration in a solid-state amplifier or oscillator.

1 Introduction

When a slow electromagnetic wave interacts with drifting electrons, its energy can grow. This principle is used to amplify and generate electromagnetic waves in velocity-modulated devices. Two examples of such devices are the traveling-wave tube and the backward-wave oscillator where an electron beam in vacuum interacts with an electromagnetic wave slowed down by a helix. Since the advent of the velocity-modulated devices in 1940s, their frequencies have gradually increased and span now three decades from about 1 GHz to 1.5 THz, the latter achieved in commercial vacuum backward-wave oscillators [1].

Further increase of the frequency in vacuum devices has met difficulties, one of them being low electron concentration (10^6–10^9 cm^{-3} [2]) resulting in low plasma frequencies. A possible solution is to replace vacuum beams with semiconductor plasmas offering higher electron concentrations. In GaAs, for example, achievable electron concentrations of 10^{15}–10^{19} cm^{-3} [3] correspond to the plasma frequencies between 350 GHz and 35 THz.

The first solid-state travelling-wave-type active device was the acoustic-wave amplifier where electrons in a piezoelectric solid interacted with acoustic waves in the MHz region [4,5]. A logical extension was the solid-state traveling-wave amplifier [6–8]. Proposals were also made for an amplifier based on the interaction between drifting electrons and optical phonons [9–11]; the idea has been recently revisited by Riyopoulos [12,13]. Mikhailov considered the interaction between drifting solid-state plasmas and quantum-wire gratings [14]. Terahertz oscillators based on semiconductor plasmas drifting in confined two-dimensional channels were studied theoretically [15] and experimentally [16].

Although solid-state plasmas offer the advantage of high frequencies, there are also drawbacks. One of them is electron collisions, absent in vacuum beams but present in solids. An obvious detrimental effect of collisions is to reduce gain. Another effect, important for practical applications, is on plasma instabilities. Instabilities can be of two types: absolute and convective [5,17,18]. For a convective instability, a signal grows in time while propagating along the structure. For an absolute instability, the signal grows in time from a seed at a particular point in space (Fig. 1). From the device perspective, absolute instabilities lead to oscillators; convective instabilities, to amplifiers.

In collision-less vacuum devices, absolute and convective instabilities are signaled by the group velocities of the waves. The convective instability of the traveling-wave tube is due to the *forward* electromagnetic wave interacting with a forward space-charge wave of the electron beam. The absolute instability of the backward-wave oscillator, on the other hand, is due to the *backward* electromagnetic wave.

In solid-state devices with collisions, the group velocities are no longer sufficient to indicate absolute and

[a] e-mail: osydoruk@imperial.ac.uk

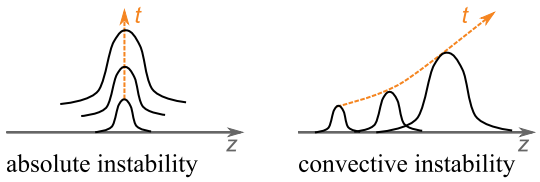

Fig. 1. (Color online) For absolute instability, a signal grows in time remaining at the place where it appeared. For convective instability, the perturbation grows in time while propagating along the structure.

convective instabilities. To analyze the instabilities and, thus, to determine practical prospects of various solid-state configurations, a careful study involving rigorous criteria [5,17,18] is required.

This paper discusses the instabilities arising from interactions between slow electromagnetic waves and drifting plasmas in the presence of collisions. We emphasize that although the rigorous criteria for instabilities [5,17,18] have been around for a long time, they have not been applied to active high-frequency devices in the presence of collisions. From a practical point of view, for designing any experiments, it is imperative to know the type of instability that will occur. We shall present an analysis based on a two-wave model that, being mathematically simple, describes a wide range of phenomena. In Section 2 we formulate the dispersion relation; in Section 3, we describe criteria for the existence of instabilities; in Section 4, we apply these criteria to the dispersion relation. We divide the treatment into four parts: the space charge wave is a forward wave, but it may propagate under low collisions and high collisions, and the circuit wave may be forward or backward. We also investigate the effect of the phase of the coupling coefficient. In Section 5, we draw conclusions.

2 Formulation of the dispersion relation

Our aim is to derive a simple dispersion equation that takes collisions into account. We start with electrons drifting along the z-axis in an infinite medium and disregard the effects of magnetic fields, i.e. when the electronic contribution is carried by cyclotron waves rather than space-charge waves. The only field component is E_z, the longitudinal component of the electric field. The relevant Maxwell equation is then

$$J_z + \varepsilon \frac{\partial E_z}{\partial t} = 0. \tag{1}$$

Here, t is time, ε is the permittivity of the material, and J_z is the current, $J_z = env$, where e is the electron charge, n is the electron density, and v is the electron velocity. We also need the equation of motion that takes collisions into account

$$\frac{dv}{dt} + v\gamma = \frac{e}{m}E, \tag{2}$$

where γ is the collision frequency, and m is the electron mass. Next, we assume that E_z, v, and n have constant parts and small time-varying parts

$$(E_z, n, v) = (E_{z0},\, n_0,\, v_0) + (\tilde{E}_z,\, \tilde{n},\, \tilde{v})\exp(\mathrm{j}\omega t),$$

where ω is the frequency, j is the complex unity, and quantities with index 0 are constants. Substituting this into equations (1) and (2), neglecting products of small quantities, using Poisson's equation, and introducing the wave number k_z with the relation $\exp(-\mathrm{j}k_z z)$, we obtain the dispersion relation in the form

$$(\omega - k_z v_0)^2 - \mathrm{j}\gamma(\omega - k_z v_0) = \omega_\mathrm{p}^2, \tag{3}$$

where ω_p is the plasma frequency $\omega_\mathrm{p}^2 = e^2 n_0/(\varepsilon m)$. Solving equation (3) for the wave number, we obtain

$$k_{z1} = \frac{1}{v_0}\left(\omega - \mathrm{j}\frac{\gamma}{2} + \omega_\mathrm{p}\sqrt{1 - \frac{\gamma^2}{4\omega_\mathrm{p}^2}}\right), \tag{4}$$

and

$$k_{z2} = \frac{1}{v_0}\left(\omega - \mathrm{j}\frac{\gamma}{2} - \omega_\mathrm{p}\sqrt{1 - \frac{\gamma^2}{4\omega_\mathrm{p}^2}}\right). \tag{5}$$

In the absence of collisions, equation (4) represents the slow space-charge wave and equation (5), the fast space-charge wave. In vacuum tubes, the slow space-charge wave is responsible for instabilities, whereas the fast space-charge wave leads to passive interactions [2]. In the model we are aiming at, the fast wave can be disregarded. Another simplification is disregarding diffusion, which, again, does not fundamentally influence the operation of velocity-modulated devices.

Next, we consider the dispersion relation for the slow electromagnetic wave (often called the circuit wave). We take it in the form of the linear dependence

$$k_z = \frac{\omega + \omega_\mathrm{s}}{v_\mathrm{s}}, \tag{6}$$

where ω_s is a constant and v_s is the group velocity. For practical circuit waves with more complicated dispersion relations, equation (6) can be regarded as the first-order series expansion of the dispersion relation.

Equations (4) and (6) represent the uncoupled dispersion relations for the slow space-charge wave and the circuit wave. They interact when coupled to each other. The coupled-wave dispersion relation can be written as

$$\left[k_z - \frac{1}{v_0}\left(\omega - \mathrm{j}\frac{\gamma}{2} + \omega_\mathrm{p}\sqrt{1 - \frac{\gamma^2}{4\omega_\mathrm{p}^2}}\right)\right]\left[k_z - \frac{\omega + \omega_\mathrm{s}}{v_\mathrm{s}}\right] = C\exp(\mathrm{j}\Phi), \tag{7}$$

where $C\exp(\mathrm{j}\Phi)$ is the coupling coefficient, which we assume to be complex. It is convenient to introduce the normalized parameters

$$\begin{aligned} K &= \frac{k_z v_0}{\omega_\mathrm{p}}, \quad \Omega = \frac{\omega}{\omega_\mathrm{p}}, \quad \Gamma = \frac{\gamma}{\omega_\mathrm{p}}, \\ \Omega_\mathrm{s} &= \frac{\omega_\mathrm{s}}{\omega_\mathrm{p}}, \quad \beta = \frac{v_0}{v_s}, \quad A = \frac{v_0^2}{\omega_\mathrm{p}^2}C. \end{aligned} \tag{8}$$

The normalized dispersion relation is then

$$\left[K-\left(\Omega-\mathrm{j}\frac{\Gamma}{2}+\sqrt{1-\frac{\Gamma^2}{4}}\right)\right]\left[K-\beta(\Omega+\Omega_\mathrm{s})\right]= A\exp(\mathrm{j}\Phi). \quad (9)$$

In Section 4, we analyze the instabilities born by this dispersion relation.

As a complex function, the normalized wave number $K(\Omega)$ has two branches. The branch points (the complex values of Ω at which the values of two branches of K merge [5,17,18]) are

$$\Omega_{\mathrm{br}\,1,2}=\frac{1}{1-\beta} \times\left[\beta\Omega_\mathrm{s}+\mathrm{j}\frac{\Gamma}{2}-\sqrt{1-\frac{\Gamma^2}{4}}\pm\sqrt{A}\exp\left(\mathrm{j}\frac{\Phi+\pi}{2}\right)\right]. \quad (10)$$

These are used for identifying absolute instabilities as discussed in the next section.

3 Formulation of the criteria for instabilities

An unstable system can be easily identified from the dispersion relation (9): one has to show that for real values of the wave number, K, solutions for the frequency, Ω, exist for which $\mathrm{Im}\,\Omega<0$. A problem more complicated is to determine the instability type. As mentioned in the introduction, there are two types of instabilities, absolute and convective, differing in spatial behavior, see Figure 1. The instability type can be determined from the criterion for absolute instability [5,17,18], see Section 3.1. On the other hand, $\mathrm{Im}\,K<0$ does not necessarily mean spatial growth (just as $\mathrm{Im}\,K>0$ does not mean decay). To determine whether solutions for $K(\Omega)$ represent growing or decaying waves, one can apply the criterion for spatial growth [5,17,18], see Section 3.2.

3.1 Criterion for absolute instability

To apply this criterion, one solves the dispersion relation 9 for K assuming complex Ω. The instability will be absolute if the following conditions are met:

1. For $\mathrm{Im}\,\Omega\to-\infty$, the solutions $\mathrm{Im}\,K_1$ and $\mathrm{Im}\,K_2$ have opposite signs.
2. The imaginary part of one of the branch points (10) is negative.

The first condition means that the uncoupled slow space-charge wave (4) and the circuit wave (6) propagate in opposite directions. Because the space-charge wave is a forward wave, absolute instability can occur only if the circuit wave is a backward wave.

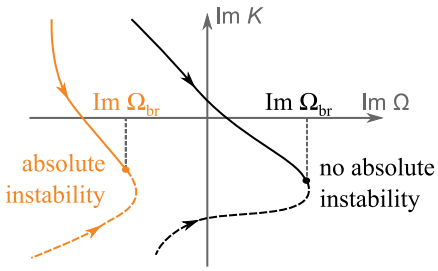

Fig. 2. (Color online) Absolute instability can be identified by plotting $\mathrm{Im}\,K$ versus $\mathrm{Im}\,\Omega$. There is absolute instability if the trajectories merge in the left half-plane but not if they merge in the right half-plane.

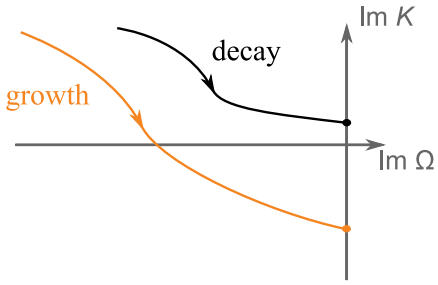

Fig. 3. (Color online) Spatial growth can be identified by plotting $\mathrm{Im}\,K$ versus $\mathrm{Im}\,\Omega$. If a trajectory crosses the $\mathrm{Im}\,K=0$ axis, the wave will grow in space.

A way to illustrate this criterion is to plot $\mathrm{Im}\,K$ versus $\mathrm{Im}\,\Omega$ fixing $\mathrm{Re}\,\Omega=\mathrm{Re}\;\Omega_\mathrm{br}$ and changing $\mathrm{Im}\,\Omega$ from $-\infty$ to $\mathrm{Im}\,\Omega_\mathrm{br}$, see Figure 2. For an absolute instability, one of the trajectories starts in the upper and the other one, in the lower half-plane, and they merge at a negative value of $\mathrm{Im}\,\Omega$.

3.2 Criterion for spatial growth

Spatial growth, corresponding to a convective instability, can only occur when there is no absolute instability [5,17,18]. Once that is ascertained, the criterion for spatial growth may be obtained from the solution of the dispersion equation (9) for $K(\Omega)$. Spatial growth is present for a particular value of $\mathrm{Re}\,\Omega$ if $\mathrm{Im}\,K$ changes sign while $\mathrm{Im}\,\Omega$ varies from $-\infty$ to 0. The criterion can again be represented by plotting $\mathrm{Im}\,K$ versus $\mathrm{Im}\,\Omega$. If the trajectory of $\mathrm{Im}\,K$ starts and ends on different sides of the $\mathrm{Im}\,K=0$ axis (see Fig. 3) the wave will grow in space.

4 Analysis of the dispersion relation

This section analyzes the dispersion relation (9) by applying the criteria for absolute instability and spatial growth. The dispersion relation depends on five parameters, Γ, β, Ω_s, A, and Φ, and even in the simple two-wave model, the

Table 1. Values of the parameters used in calculations.

	Low collision frequency		High collision frequency	
	Forward circuit wave	Backward circuit wave	Forward circuit wave	Backward circuit wave
Γ	0.1	0.1	10	10
A	0.05	0.05	0.001	0.001
Φ	π	0	$\pi/2$	$3\pi/2$
β	2	-2	2	-2
Ω_s	0	2	0	2

number of possible combinations is enormous. For this reason, rather than attempt a general analysis, we consider only representative combinations (see Tab. 1).

The first parameter is the normalized collision frequency, Γ. In semiconductors with collision frequencies in the range 1–30 THz and plasma frequencies in the range 0.5–50 THz [3,19], Γ can be as low as 0.02 and as high as 60. Most practically significant are the configurations with low collision frequencies (high plasma frequencies, low temperatures) and with high collision frequencies (low plasma frequencies, room temperatures). We focus, therefore, on the values $\Gamma = 0.1$ (Sect. 4.1) and $\Gamma = 10$ (Sect. 4.2).

The second parameter is the coupling coefficient. Its absolute value, A, determines the interaction strength. The two-wave model, equation (9), implies weak interaction, $A \ll 1$; one also expects greater values of A at low collision frequencies than at high collision frequencies. We take, therefore, $A = 0.05$ for the former and $A = 0.001$ for the latter case. The phase of the coupling coefficient, Φ, takes values 0, $\pi/2$, π and $3\pi/2$ in, respectively, the dispersion relations of the backward-wave oscillator [2], the acoustic-wave amplifier [4,5], the traveling-wave tube [2], and the optical-phonon amplifier [10,11]. These values correspond to either purely real or purely imaginary positive and negative coupling coefficients. In general, however, due to collisions, the coupling coefficient can be complex, as for example in the resistive medium amplifier [20]. We will, therefore, investigate the whole range of values $0 < \Phi < 2\pi$.

The remaining parameters, β and Ω_s, characterize the circuit wave. As Section 3 shows, the instability type depends on whether the circuit wave is a forward or a backward wave. We take $\beta = 2$ and $\Omega_s = 0$ for forward circuit waves and $\beta = -2$ and $\Omega_s = 2$ for backward circuit waves, so that the interaction frequencies for both lie around $\Omega = 1$ ($\omega = \omega_p$).

4.1 Instabilities at low collision frequencies

For low collision frequencies, $\Gamma \ll 1$, the dispersion relation (9) simplifies to

$$\left[K - \left(\Omega + 1 - j\frac{\Gamma}{2}\right)\right][K - \beta(\Omega - \Omega_s)] = A\exp(j\Phi). \tag{11}$$

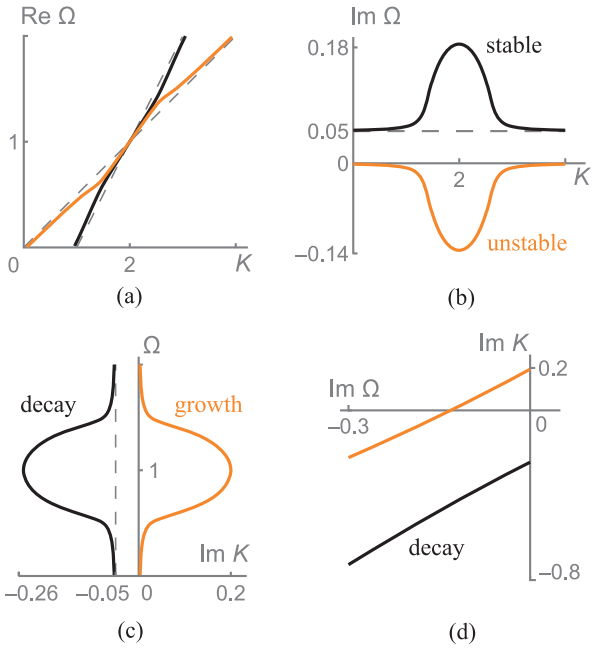

Fig. 4. (Color online) Dispersion diagrams for $\Omega(K)$ and $K(\Omega)$ (a)–(c) show the presence of instability and spatial growth when drifting electrons with low collision frequency ($\Gamma = 0.1$) interact with a forward circuit wave. Criterion for spatial growth (d) confirms amplification of the circuit wave.

Below, we consider the instabilities arising from the interaction with forward circuit waves ($\beta > 0$) and with backward circuit waves ($\beta < 0$).

Forward circuit waves

Using the parameters from the first column of Table 1, the dispersion equation for complex $\Omega(K)$ versus real K is plotted in Figures 4a and 4b. One of the branches of the dispersion diagram has $\mathrm{Im}\,\Omega < 0$ indicating an instability. It is a convective instability, because the waves propagate in the same direction. Convective instability leads to spatial growth. To determine the rate of growth, we solve the dispersion equation for $K(\Omega)$ where K is complex and Ω is real. In one of the solutions, $\mathrm{Im}\,K > 0$, see Figure 4c. The imaginary parts of Ω and K characterize the rates of temporal and spatial growth. Both have their maxima at the synchronism point, where the phase velocities of the uncoupled waves coincide and the uncoupled dispersion relations cross, as shown in Figure 4a by dashed lines.

The criterion of Section 3.2 provides further confirmation of spatial growth. To apply the criterion, we take $\mathrm{Re}\,\Omega = 1.1$ and plot $\mathrm{Im}\,K$ versus $\mathrm{Im}\,\Omega$ in Figure 4d. As $\mathrm{Im}\,\Omega$ changes from a negative value to zero, one of the trajectories for K crosses the $\mathrm{Im}\,K = 0$ axis. The value of $\mathrm{Im}\,K$ at $\mathrm{Im}\,\Omega = 0$ gives the normalized growth rate.

The growth rate depends also on the phase of the coupling coefficient. Figure 5 shows $\max(\mathrm{Im}\,K)$ as a function of the phase, Φ. The maximum occurs at $\Phi = \pi$, corresponding to the real negative coupling coefficient we chose

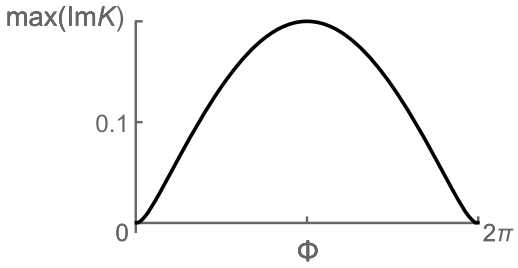

Fig. 5. The growth rate depends on the phase of the coupling coefficient. There is no growth for phases close to 0 and 2π.

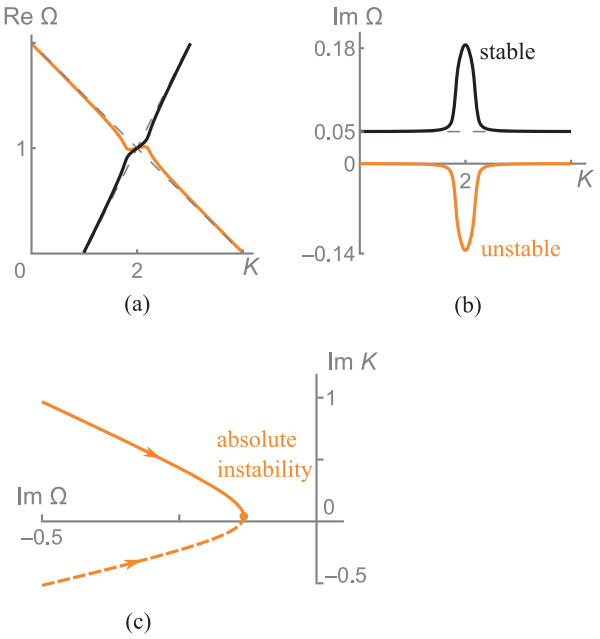

Fig. 6. (Color online) Dispersion diagrams for $\Omega(K)$ and $K(\Omega)$ (a)–(b) show the presence of instability when drifting electrons with low collision frequency ($\Gamma = 0.1$) interact with a backward circuit wave. The instability is absolute (c).

above. The gain is absent not only for $\Phi = 0$ and 2π but also for narrow regions in their vicinity.

Backward circuit waves

Using the parameters from the second column of Table 1, the solutions of the dispersion relation are plotted in Figures 6a and 6b for the real and imaginary parts of Ω assuming real K. In one of the branches, $\mathrm{Im}\,\Omega < 0$ indicating, again, an instability. The rate of temporal growth, $|\mathrm{Im}\,\Omega|$, reaches maximum at the synchronism point.

The two branch points, equation (10), are $\Omega_{\mathrm{br}\,1} = 1.00 + 0.17\mathrm{j}$ and $\Omega_{\mathrm{br}\,2} = 1.00 - 0.13\mathrm{j}$. The second one, lying in the lower part of the complex Ω-plane, satisfies the first condition for absolute instability, see Section 3.1. The second condition involves mapping of the line $\Omega = \mathrm{Re}\,\Omega_{\mathrm{br}\,2} + \mathrm{j}\,\mathrm{Im}\,\Omega$, with $\mathrm{Im}\,\Omega$ varying from $-\infty$ to $\mathrm{Im}\,\Omega_{\mathrm{br}\,2}$, upon the complex K-plane. The two solutions for complex K emerge from different sides of the complex K-plane and converge upon the branch point, for which $\mathrm{Im}\,\Omega$ is negative, Figure 6c.

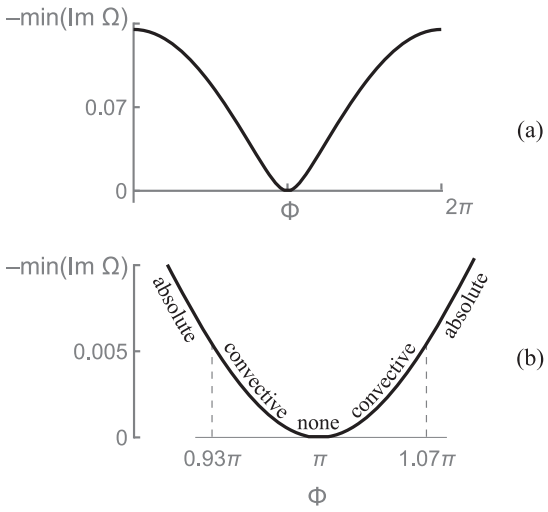

Fig. 7. The rate of temporal growth and the type of instability depend on the phase of the coupling coefficient.

The type of instability depends on the magnitude of the coupling coefficient [18]. The transition from absolute to convective instability occurs when the imaginary parts of both branch points become non-negative. From equation (10), the condition is

$$A < \frac{\Gamma^2}{16}. \tag{12}$$

With our parameters, it occurs when $A < 6.25 \times 10^{-4}$.

As may be expected, the temporal rate of growth depends on the phase of the coupling coefficient. Figure 7a shows the variation of $-\min(\mathrm{Im}\,\Omega)$ for $A = 0.05$. The maxima occur at $\Phi = 0$ and 2π. In the vicinity of $\Phi = \pi$ the behavior is different, as shown in Figure 7b. As Φ approaches π, the absolute instability first turns into convective instability and then into no instability at all, and the other way round as Φ increases beyond the value of π. The disappearance of the absolute instability follows from equation (10). The imaginary parts of both branch points turn non-negative when

$$\cos\frac{\Phi}{2} < \frac{\Gamma}{4\sqrt{A}}. \tag{13}$$

For our parameters chosen, there is no absolute instability for $0.93\pi < \Phi < 1.07\pi$.

4.2 Instabilities at high collision frequencies

The dispersion equation (9) for high collision frequency simplifies to

$$\left[K - \left(\Omega - \mathrm{j}\frac{1}{\Gamma}\right)\right][K - \beta(\Omega - \Omega_{\mathrm{s}})] = A\exp(\mathrm{j}\Phi). \tag{14}$$

This dispersion relation differs from the low-collision one, equation (11), in one important respect. The loss term

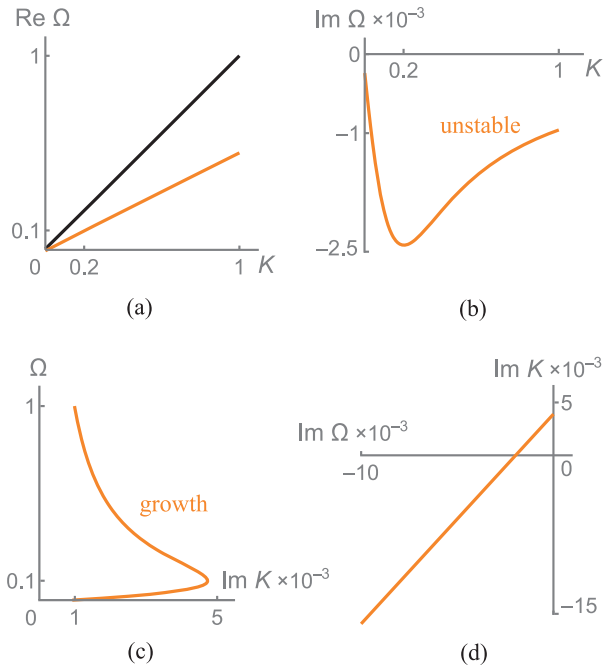

Fig. 8. (Color online) Dispersion diagrams for $\Omega(K)$ and $K(\Omega)$ (a)–(c) show the presence of instability and spatial growth when drifting electrons with large collision frequency ($\Gamma = 10$) interact with a forward circuit wave. Criterion for spatial growth (d) confirms amplification of the circuit wave.

$1/\Gamma$ in equation (14) declines as the collision frequency increases. This may sound as a paradox: collisions are usually associated with losses. At the other end of the scale, however, high collisions mean that the electrons have no chance to accelerate to high velocities, and therefore, the conductivity, $\sigma = \omega_p^2/\gamma$, declines – and it is the conductivity that determines the loss.

Forward circuit waves

The dispersion diagrams for $\mathrm{Re}\,\Omega(K)$ and for $\mathrm{Im}\,\Omega(K)$ are shown in Figures 8a and 8b for the parameters from the third column of Table 1. There are two solutions, but we have shown in Figure 8b only the one for which $\mathrm{Im}\,\Omega < 0$ indicating, again, an instability. It is of the convective type, because the interaction is between two forward waves. The circuit wave grows in space as may be seen from the solution for $\mathrm{Im}\,K(\Omega)$ presented in Figure 8c: $\mathrm{Im}\,K$ may be larger than zero. The rigorous criterion for spatial growth may be gleaned from Figure 8d. We take $\mathrm{Re}\,\Omega = 0.2$ and change $\mathrm{Im}\,\Omega$ from a large negative value to zero. As seen from the $\mathrm{Im}\,K$ versus $\mathrm{Im}\,\Omega$ diagram, $\mathrm{Im}\,K$ changes sign as $\mathrm{Im}\,\Omega$ reaches zero.

Similarly to the low-collision-frequency regime, the growth rate depends on the phase of the coupling coefficient, Φ, but this dependence is now stronger. Figure 9 shows the variation of $\max(\mathrm{Im}\,K)$ for $A = 0.001$ with Φ changing from 0 to 2π. The growth is maximum for $\Phi = \pi$. There is no growth for $1.5\pi < \Phi < 2\pi$ and for Φ close to zero.

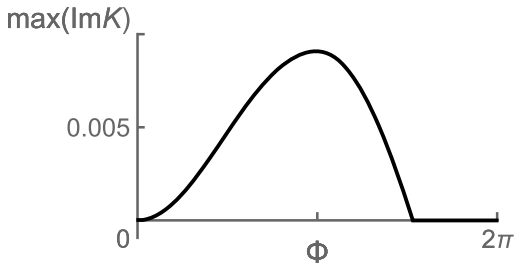

Fig. 9. The maximum growth rate depends on the phase of the coupling coefficient. The growth disappears for phases larger than $3\pi/2$.

Backward circuit waves

The solutions of the dispersion equation $\Omega(K)$ for real K are shown in Figures 10a and 10b for the parameters from the fourth column of Table 1. In the backward-wave branch, $\mathrm{Im}\,\Omega < 0$ for $K > 1.33$. The instability region has thus a low-wave number cut-off, in contrast to previous examples.

Applying the criterion of Section 3.1, we find no absolute instability. Both branch points have positive imaginary parts: $\Omega_{\mathrm{br}\,1} = 1.35 + 0.05\mathrm{j}$ and $\Omega_{\mathrm{br}\,2} = 1.32 + 0.02\mathrm{j}$. In Figure 10c, $\mathrm{Im}\,K$ is plotted versus $\mathrm{Im}\,\Omega$ for $\mathrm{Re}\,\Omega = \mathrm{Re}\,\Omega_{\mathrm{br}\,2}$. Although the trajectories for K start in different half-planes of complex K, both branch points are in the upper half-plane of complex Ω. The backward wave is expected to grow in space for $\Omega < 1.33$, where $\mathrm{Im}\,K < 0$, as suggested by the dispersion diagram for $K(\Omega)$, Figure 10d. Similarly to the solutions for $\Omega(K)$, the growing-wave region also has a cut-off, but at high frequency.

Spatial growth of the backward wave at low frequencies is confirmed by the criterion of Secetion 3.2. For $\mathrm{Re}\,\Omega = 1.3$, the trajectory of K corresponding to the backward wave crosses the axis $\mathrm{Im}\,K = 0$ as $\mathrm{Im}\,\Omega$ changes from a large negative value to zero, see Figure 10e. For $\Omega > 1.33$ neither of the two trajectories of K crosses the $\mathrm{Im}\,K = 0$ axis; hence, there is no spatial growth at those frequencies.

If the collision frequency, Γ, increases, the loss $1/\Gamma$ decreases, and the instability can turn from convective to absolute. The transition occurs when the imaginary part of one of the branch points, equation (10), becomes negative. For $\Phi = 3\pi/2$, this condition is

$$\Gamma > \frac{1}{\sqrt{2A}}. \tag{15}$$

We demonstrate the effects of higher collision frequency by taking $\Gamma = 50$ and keeping the remaining parameters from the previous example. The dispersion diagrams for $\Omega(K)$ are shown in Figures 11a and 11b. The real part of Ω is more or less the same as in Figure 10a but for a small gap. The curves for the imaginary part of Ω are quite different. There is now a point at which $\mathrm{Im}\,\Omega$ changes abruptly. Negative imaginary values of Ω for one of the branches indicate instability. The instability is absolute, as shown in Figure 11c. One of the branch points has $\mathrm{Im}\,\Omega_{\mathrm{br}} < 0$, and the curves merge from different sides of the K-plane.

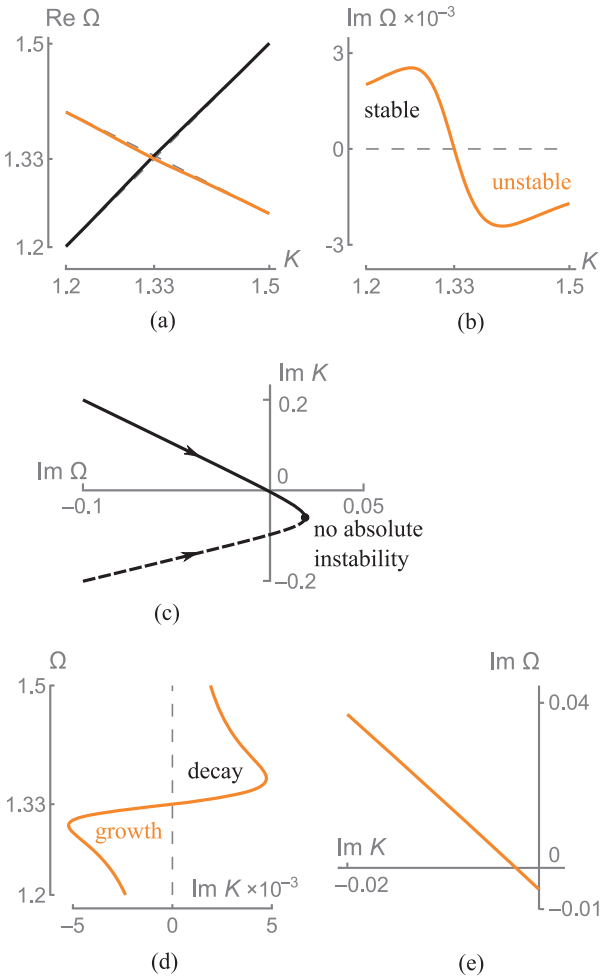

Fig. 10. (Color online) Dispersion diagrams for $\Omega(K)$ (a)–(b) show the presence of instability when drifting electrons with moderate collision frequency ($\Gamma = 10$) interact with a backward circuit wave. The instability is convective (c); the presence of spatial growth is confirmed by the dispersion diagram for $K(\Omega)$ (d) and by the corresponding criterion (e).

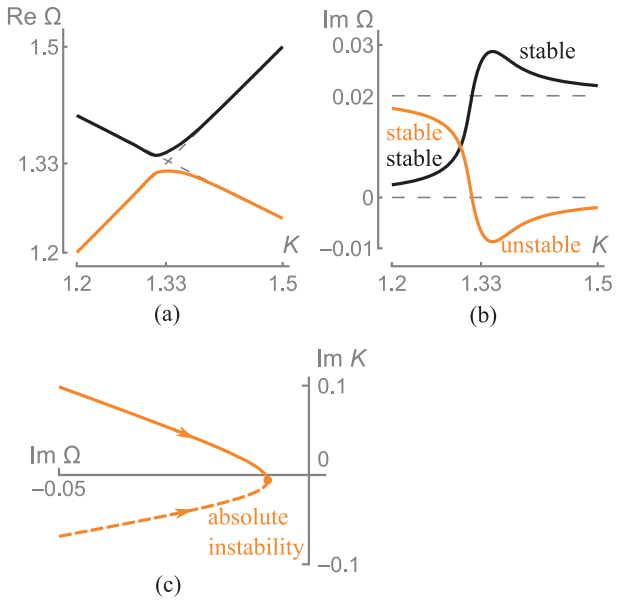

Fig. 11. (Color online) Dispersion diagrams for $\Omega(K)$ (a)–(b) show the presence of instability when drifting electrons with high collision frequency ($\Gamma = 50$) interact with a backward circuit wave. The instability is absolute (c).

5 Conclusions

Applying the rigorous instability criteria to the two-wave dispersion relation, we determined when the interaction between drifting solid-state plasmas and circuit waves lead to absolute and convective instabilities. This model is general, and being applied to a particular configuration, it can identify whether this configuration has potential for a solid-state traveling-wave amplifier or oscillator.

As the analysis showed, the dispersion relation at low collision frequencies behaves similarly to the collisionless dispersion relation: under certain conditions, forward circuit waves lead to convective instabilities; backward circuit waves, to absolute instabilities. There are also differences. When the phase of the coupling coefficient changes in the presence of collisions, an absolute instability may turn into a convective one and then to no instability at all; there is no such effect in the absence of collisions.

Low collision frequencies, however, might not always be practically attainable. The normalized collision frequency could be high, for example, at room temperatures or at lower plasma frequencies. Depending on the relationship between the collision frequency and the coupling coefficient, the instability can be either convective or absolute, with absolute instability occurring at higher collision rates. Somewhat surprisingly, high collisions turned out to be beneficial for absolute instability and, hence, for a THz oscillator, which could be based, for example, on optical phonons [12,13].

We thank R. R. A. Syms for helpful discussions. O. S. acknowledges financial support by the Royal Society and the Royal Academy of Engineering (Newton International Fellowship). E. S. acknowledges financial support by the German Research Foundation (SAOT and Emmy Noether-Programme).

References

1. H.B. Liu, H. Zhong, N. Karpowicz, Y. Chen, X.C. Zhang, Proc. IEEE **95**, 1514 (2007)
2. R.E. Collin, *Foundations for Microwave Engineering* (Wiley-IEEE Press, Hoboken, New Jersey, 2001)
3. M. Shur, *GaAs Devices and Circuits* (Plenum Press, New York, 1987)
4. A.R. Hutson, J.H. McFee, D. White, Phys. Rev. Lett. **7**, 237 (1961)

5. M.C. Steel, B. Vural, *Wave Interactions in Solid State Plasmas* (McGraw-Hill, New York, 1969)
6. L. Solymar, E.A. Ash, Int. J. Electron. **20**, 127 (1966)
7. M. Sumi, Appl. Phys. Lett. **9**, 251 (1966)
8. M. Sumi, T. Suzuki, Appl. Phys. Lett. **13**, 326 (1968)
9. V.L. Gurevich, Sov. Phys. Solid State **4**, 1015 (1962)
10. J.B. Gunn, Phys. Lett. **4**, 194 (1963)
11. L. Solymar, The coupled modes of interacting optical phonons and drifting electrons, in *Proc. of the 5th International Congress of Microwave Tubes* (Paris, 1964), p.501
12. S. Riyopoulos, Phys. Plasmas **12**, 070704 (2005)
13. S. Riyopoulos, Phys. Plasmas **16**, 033103 (2009)
14. S.A. Mikhailov, Phys. Rev. B **58**, 1517 (1998)
15. M. Dyakonov, M. Shur, Phys. Rev. Lett. **71**, 2465 (1993)
16. A. El Fatimy, N. Dyakonova, Y. Meziani, T. Otsuji, W. Knap, S. Vandenbrouk, K. Madjour, D. Theron, C. Gaquiere, M.A. Poisson et al., J. Appl. Phys. **107**, 024504 (2010)
17. R.J. Briggs, *Electron-Stream Interaction with Plasmas, Research Monograph No. 29* (M.I.T. Press, Cambridge, Massachusetts, 1964)
18. A.M. Fedorchenko, N.I. Kotsarenko, *Absolute and convective instabilities in plasmas and solids* (Izdatel'stvo Nauka, Moscow, 1981), in Russian
19. T.H. Isaac, J.G. Rivas, J.R. Sambles, W.L. Barnes, E. Hendry, Phys. Rev. B **77**, 113411 (2008)
20. B. Vural, S. Bloom, IEEE Trans. Electron Devices **ED-14**, 345 (1967)